Monte-Carlo Simulation of Solar Active-Region Energy

M.S. Wheatland[1]

Abstract A Monte-Carlo approach to solving a stochastic jump transition model for active-region energy (Wheatland and Glukhov, *Astrophys. J.* **494**, 1998; Wheatland, *Astrophys. J.* **679**, 2008) is described. The new method numerically solves the stochastic differential equation describing the model, rather than the equivalent master equation. This has the advantages of allowing more efficient numerical solution, the modelling of time-dependent situations, and investigation of details of event statistics. The Monte-Carlo approach is illustrated by application to a Gaussian test case, and to the class of flare-like models presented in Wheatland (2008), which are steady-state models with constant rates of energy supply, and power-law distributed jump transition rates. These models have two free parameters: an index (δ), which defines the dependence of the jump transition rates on active-region energy, and a non-dimensional ratio ($\overline{r}$) of total flaring rate to rate of energy supply. For $\overline{r} \ll 1$ the non-dimensional mean energy $\langle \overline{E} \rangle$ of the active-region satisfies $\langle \overline{E} \rangle \gg 1$, resulting in a power-law distribution of flare events over many decades in energy. The Monte-Carlo method is used to explore the behavior of the waiting-time distributions for the flare-like models. The models with $\delta \neq 0$ are found to have waiting times which depart significantly from simple Poisson behavior when $\langle \overline{E} \rangle \gg 1$. The original model from Wheatland and Glukhov (1998), with $\delta = 0$ (no dependence of transition rates on active-region energy), is identified as being most consistent with observed flare statistics.

Keywords: Active Regions, Models; Corona, Models; Flares, Models; Flares, Microflares and Nanoflares

1. Introduction

Solar flares are explosive events in the solar corona, involving the release of energy stored in active-region magnetic fields. Active regions are dynamic, evolving in time due to the emergence and submergence of magnetic flux from the sub-photosphere, stressing by photospheric motions, and the occurrence of flares. It is of interest to understand the dynamical energy balance of active regions.

[1] School of Physics, University of Sydney, NSW 2006, Australia
email: m.wheatland@physics.usyd.edu.au

Flares exhibit a wide range of energies. The largest flares may involve the release of up to 10^{27} J of energy, and are associated with large-scale expulsions of material from the corona (Coronal Mass Ejections, or CMEs), involving comparable energies. Small flare-like events are observed down to the limits of observation and are difficult to distinguish from a variety of small-scale solar activity. The distribution of flare energies follows a power-law distribution (Hudson, 1991; Crosby, Aschwanden, and Dennis, 1993; Aschwanden, Dennis, and Benz, 1998). Specifically, the frequency-energy distribution $\mathcal{N}(E)$, *i.e.* the number of flares observed per unit time and per unit energy (E), obeys

$$\mathcal{N}(E) = AE^{-\gamma}, \tag{1}$$

where the factor A is a (time-dependent) measure of the total flaring rate, and $\gamma \approx 1.5$. This distribution is often constructed for flares from all active regions present on the Sun over some period of time, but it also appears to apply to individual active regions (Wheatland, 2000), which suggests that the power law is fundamental to the flare mechanism. A popular model explaining the power law is the avalanche model (Lu and Hamilton, 1991; Charbonneau *et al.*, 2001), in which the magnetic field in the corona is assumed to be in a self-organized critical state, and subject to avalanches of small-scale reconnection events. The distribution (1) must have an upper roll-over, to ensure that the total energy released in flares is finite (Kucera *et al.*, 1997; Hudson, 2007).

The mechanisms causing flares are not well understood, and flares appear to occur randomly in time, although certain properties of active regions correlate with flaring (*e.g.* Sammis, Tang, and Zirin, 2000; McIntosh, 1990; Georgoulis and Rust, 2007; Schrijver, 2007). Correspondingly, the prediction of flares is in its infancy: the methods used are probabilistic and are rather inaccurate at predicting the occurrence of large flares, which are rare but which strongly influence our local space weather (Wheatland, 2005; Barnes *et al.*, 2007; Barnes and Leka, 2008).

The occurrence of flares in time may be investigated via a second observable distribution, the flare waiting-time distribution, or the distribution of times between events (this distribution is also referred to as the "interval distribution"). Determinations of flare waiting-time distributions have given varied results (Pearce, Rowe, and Yeung, 1993; Biesecker, 1994; Wheatland, Sturrock, and McTiernan, 1998; Boffetta *et al.*, 1999; Lepreti, Carbone, and Veltri, 2001; Moon *et al.*, 2001; Wheatland, 2001; Moon *et al.*, 2002; Kubo, 2008), suggesting that the observed distribution may depend on the particular active region, on time, and that it also may be influenced by event definition and selection procedures (Wheatland, 2001; Buchlin, Galtier, and Velli, 2005; Paczuski, Boettcher, and Baiesi, 2005; Baiesi, Paczuski, and Stella, 2006). For some active regions, the distribution is consistent with a simple Poisson process, *i.e.* independent events occurring at a constant mean rate (Moon *et al.*, 2001), and the corresponding waiting-time distribution is exponential. Other active regions exhibit time-variation in the flaring process, and flare occurrence may be approximated by a piecewise-constant, or more generally time-varying Poisson process, in which case the distribution is a sum or integral over exponentials (Wheatland,

2001). On longer time scales, the distribution exhibits a power-law tail for events from the whole Sun (Boffetta *et al.*, 1999). Some authors have also argued that the process is fundamentally non-Poissonian (*e.g.* Lepreti, Carbone, and Veltri, 2001), although the arguments neglect the role of time-dependence.

The energy balance of active regions presents a puzzle, because of the large drops in energy due to large solar flares. In the following we consider a simple "black box" approach to modelling the free energy of an active region (the energy available to power flares), an approach that goes back to Rosner and Vaiana (1978). Energy is assumed to be continuously supplied to the active region by some external mechanism. The energy is stored locally in the corona, and some is released at particular times in flares. The flaring process is considered to be stochastic, whereas energy supply is deterministic. Flares are treated as point processes in time, *i.e.* they occur at one instant in time, and they involve jump transitions (discontinuous changes) in energy. A general model of this kind was presented in Wheatland and Glukhov (1998) and further developed in Wheatland (2008). The general model is based on a master equation for the probability distribution $[P(E, t)]$ for the free energy (E) of an active region at time t. The free parameters in the model are a prescribed energy supply rate to the system $[\beta(E, t)]$, and prescribed transition rates $[\alpha(E, E', t)]$, describing the rate of jumps from energy E to energy $E' \leq E$. These two rate functions may have any functional form. In Wheatland and Glukhov (1998) it was argued that the energy-supply rate should not depend on the energy (E) of the system, since active regions are driven externally, and hence a constant energy supply rate is appropriate. It was also argued that, to produce an appropriate power-law flare frequency-energy distribution, transition rates of the form $\alpha(E, E') \sim (E - E')^{-\gamma}$ are required (in the steady state). Wheatland and Glukhov (1998) and Wheatland (2008) investigated the model by solving the master equation in the steady state, for these "flare-like" choices for the free parameters. In Wheatland and Glukhov (1998) the emphasis was on the basic model and the arguments for the appropriate flare-like choices. A model was constructed that could reproduce power-law behavior in the flare frequency-energy distribution over an arbitrary number of decades in energy, up to a high energy roll-over set by the decline of $P(E)$ at large energy. Hence the flare-like model was confirmed to reproduce this aspect of flare statistics. In Wheatland (2008) the waiting-time distributions for the model were also considered, using theory for jump transition processes presented for the first time by Daly and Porporato (2007). It was found that the Wheatland and Glukhov (1998) model produces an essentially Poisson (exponential) waiting-time distribution. A modified model was also considered, involving an $\alpha(E, E') \sim E(E - E')^{-\gamma}$ form for the transition rates. This model also reproduced the power-law frequency-energy distribution, but exhibited some departure from a simple Poisson waiting-time distribution.

Master equations may be represented by an equivalent stochastic differential equation (van Kampen, 1992; Gardiner, 2004), which provides a complementary approach to the problem at hand. Stochastic DEs are amenable to solution by Monte-Carlo methods, which in general are simple to numerically implement. This paper describes a Monte-Carlo approach to solving the stochastic model for solar active-region energy presented in Wheatland and Glukhov (1998) and

Wheatland (2008). The Monte-Carlo approach has specific advantages over the master-equation approach: it is computationally more efficient, it permits more general modelling, in particular the modelling solution of time-dependent problems, and it generates an ensemble of flare events and hence permits detailed investigation of event statistics.

The layout of the paper is as follows. The master-equation approach of Wheatland and Glukhov (1998) and Wheatland (2008) is briefly reiterated in Section 2.1, and the flare-like choices for the model are explained in Section 2.2. The stochastic DE approach to the problem is then presented in Section 3.1, and illustrated by application to a Gaussian test case (Section 3.2), and to the flare-like cases from Wheatland (2008) (Section 3.3), including comparison of a Monte-Carlo solution with direct numerical solution of the master equation. Section 3.4 presents a Monte-Carlo-based investigation of the variation of the waiting-time distribution for the flare-like models, and Section 4 presents conclusions.

2. Master Equation Approach

2.1. GENERAL APPROACH

To begin we briefly reiterate the master-equation formulation of the model, following Wheatland and Glukhov (1998) and Wheatland (2008). The energy $[E = E(t)]$ of an active region is assumed to be a stochastic variable which evolves in time due to deterministic energy input at a rate $\beta(E, t)$, as well as due to jumps downwards in energy (flares) at random times and of random sizes, described by transition rates $\alpha(E, E', t)$. These are the rate for jumps per unit energy from E to E' at time t. The probability distribution $[P(E, t)]$ for the energy of the system is given by the solution to the master equation

$$\frac{\partial P(E, t)}{\partial t} = -\frac{\partial}{\partial E}\left[\beta(E, t)P(E, t)\right] - \lambda(E, t)P(E, t)$$
$$+ \int_E^\infty P(E', t)\alpha(E', E, t)\mathrm{d}E', \tag{2}$$

where

$$\lambda(E, t) = \int_0^E \alpha(E, E', t)\mathrm{d}E' \tag{3}$$

is the total rate of flaring at time t, assuming the system has energy E. [A time dependence has been included in the transition rate, by contrast with Wheatland (2008).] Two other quantities of interest are the mean total rate of transitions (in the average over energy)

$$\langle\lambda\rangle = \int_0^\infty \lambda(E, t)P(E, t)\mathrm{d}E \tag{4}$$

and the mean energy of the system

$$\langle E \rangle = \int_0^\infty E P(E,t) \mathrm{d}E. \tag{5}$$

As noted in Section 1, two observable flare distributions are the flare frequency-energy distribution and the waiting-time distribution. The model frequency-energy distribution is given by

$$\mathcal{N}(E,t) = \int_E^\infty P(E',t)\alpha(E', E' - E, t)\mathrm{d}E'. \tag{6}$$

Daly and Porporato (2007) showed how to obtain the distribution of waiting times (τ) for jump transition models in the steady state ($\partial/\partial t = 0$). In Wheatland (2008) that theory was applied to Equation (2) to yield the model waiting-time distribution $p_\tau(\tau)$. The details of the derivation are given in Wheatland (2008).

In Wheatland and Glukhov (1998) and Wheatland (2008) the master equation was numerically solved in the steady state, for flare-like choices of $\beta(E)$ and $\alpha(E, E')$ (the choices are explained in Section 2.2). The methods of solution involved discretising the energy as a set of values E_i ($i = 1, 2, 3, ..., N$), in which case the master equation represents a system of N linear equations in N unknowns $P_i = P(E_i)$. Solution of the linear system was performed either by relaxation (Wheatland and Glukhov, 1998), or by back substitution (Wheatland, 2008). One disadvantage of these methods is that the energy may span many decades in energy, in which case a large value of N is required.

2.2. FLARE-LIKE CHOICES

In Wheatland and Glukhov (1998), the master equation was solved in the steady state ($\partial/\partial t = 0$) for the choices $\beta(E) = \beta_0$, a constant, and

$$\alpha(E, E') = \alpha_0(E - E')^{-\gamma}\theta(E - E' - E_c), \tag{7}$$

where α_0 is a constant, E_c is a low-energy cutoff, and $\theta(x)$ is the step function. In Wheatland (2008) Equation (7) was generalised to include an additional dependence on the initial energy E:

$$\alpha(E, E') = \alpha_0 E^\delta (E - E')^{-\gamma}\theta(E - E' - E_c), \tag{8}$$

where δ is a constant. The problem was solved for Equation (8) with $\delta = 0$ and $\delta = 1$, and for $\beta(E) = \beta_0$.

The physical motivations for these choices is briefly mentioned in Section 1, but is worth discussing in more detail. Concerning the energy-supply rate, the physical aspect is that the rate does not depend on the energy of the system. This is appropriate for a system that is externally driven, and for which there is no back reaction of the system on the driver. The picture for the Sun is that energy supply comes from below (*i.e.* from the sub-photosphere), *via* photospheric flows which cause new fields to emerge into the corona, and twist existing coronal

fields. The rate at which this occurs is determined by flow patterns in the sub-photosphere. The sub-photosphere is very dense, so it is unlikely that the corona can influence the rate of supply of energy, assuming this picture of energy supply is correct. Of course, the energy supply rate may depend on time, and the choice of a constant supply rate is a simplification. We will return to the question of time-dependent driving in Section 4.

Concerning the functional forms for the transition rates, first note that substituting Equation (8) into Equation (6) leads to the flare frequency-energy distribution

$$\mathcal{N}(E) = \alpha_0 E^{-\gamma} \int_E^\infty \left(E'\right)^\delta P(E') \mathrm{d}E', \tag{9}$$

for $E \geq E_c$. It follows that the frequency-energy distribution is a power law with index γ up to energies E at which $P(E)$ becomes very small. This is consistent with the observed power-law frequency-energy distribution (1), and the physical requirement that the frequency-energy distribution rolls over at large energies (to ensure the total mean rate of energy release in flares is finite). An estimate of the energy for departure from power-law behavior is provided by the mean energy, which may be approximated by (Wheatland and Glukhov, 1998)

$$\langle E \rangle \approx \left(\frac{2-\gamma}{\alpha_0/\beta_0}\right)^{1/(\delta+2-\gamma)}. \tag{10}$$

In principle, other functional choices leading to power-law behavior are possible, although it has proven difficult to identify alternative solutions with an energy-supply rate independent of energy that produce a power-law form for $\mathcal{N}(E)$.

Another motivation for the choices (7) and (8) for the transition rates comes from consideration of avalanche type models (Lu and Hamilton, 1991; Charbonneau *et al.*, 2001). In these models the volume involved in flaring is the set of unstable sites which trigger one another during the flare "avalanche." The volume of this region is found to be scale free, *i.e.* power-law distributed, and is fractal in shape. Assuming the volume of the region is proportional to the energy released, this implies a form $\sim (E - E')^{-\gamma}$ for the probability per unit time of a transition from energy E to E', assuming flares occur at a constant rate per unit time. Hence the flare-like choices for the master equation may correspond to the avalanche model, although the detailed relationship between the two pictures remains to be worked out.

Some support for these choices is provided by the resulting waiting-time distributions. The numerical solutions for $P(E)$ in Wheatland (2008) lead to waiting-time distributions which are approximately exponential. This may be understood by noting that substituting Equation (8) into Equation (3) gives the total rate for flaring

$$\lambda(E, t) = \begin{cases} \alpha_0 E^\delta \left(E_c^{-\gamma+1} - E^{-\gamma+1}\right)/(\gamma-1) & \text{if } E \geq E_c, \\ 0 & \text{else.} \end{cases} \tag{11}$$

For $E \gg E_c$ we have

$$\lambda(E) \approx \frac{\alpha_0}{\gamma-1} E_c^{-\gamma+1} E^\delta. \tag{12}$$

For $\delta = 0$, Equation (12) implies $\lambda(E)$ is constant (independent of E). For $\delta = 1$ we have $\lambda(E) \propto E$, and hence the mean rate may be approximately constant, provided $P(E)$ is non-zero only over a fairly limited range in E. Hence the total rate of flaring may be approximately constant for $\delta = 0$ and $\delta = 1$, consistent with a simple Poisson process. As discussed in Section 1, this is compatible with observed flare statistics in active regions for which the rate does not vary in time (Moon *et al.*, 2001; Wheatland, 2001).

3. Stochastic DE Approach

3.1. GENERAL APPROACH

Following Daly and Porporato (2007), the master Equation (2) is equivalent to the stochastic differential equation

$$\frac{\mathrm{d}E}{\mathrm{d}t} = \beta(E, t) - \Lambda(E, t) \tag{13}$$

where

$$\Lambda(E, t) = \sum_{i=1}^{N(t)} \Delta E_i \delta(t - t_i) \tag{14}$$

describes the loss in energy due to flaring, with $\delta(x)$ being the delta function, $N(t)$ being the number of events up to time t, and with the event times t_i defined by a "state-dependent" Poisson process with occurrence rate $\lambda(E, t)$. The jump amplitudes ΔE follow the distribution $h(\Delta E, E, t)$, defined by

$$\alpha(E, E - \Delta E, t) = \lambda(E, t)h(\Delta E, E, t), \tag{15}$$

so that

$$\int_0^E h(\Delta E, E, t)\mathrm{d}(\Delta E) = 1. \tag{16}$$

The ODE (13) may be solved in the following way. First, choose a start-energy E_s at time t_s. The energy of the system evolves deterministically from this time up until the first jump at time $t_e = t_s + \tau$, where τ is a waiting time. The waiting time corresponds to a time-dependent Poisson process with a rate $\lambda[E(t), t]$. To evaluate this rate, note that the energy during the deterministic trajectory obeys

$$\frac{\mathrm{d}E}{\mathrm{d}t} = \beta(E, t). \tag{17}$$

Solving Equation (17) with the initial condition $E = E_s$ at $t = t_s$ defines the time history $E^*(t)$ for the energy, and this together with $\lambda = \lambda(E, t)$ defines the rate $\lambda[E^*(t), t]$ prior to a jump. A waiting time may be generated for this rate by finding the root of the monotonic function (Wheatland and Craig, 2006):

$$F(\tau) = \ln(1 - u) + \int_{t_s}^{t_s + \tau} \lambda[E^*(t), t]\,\mathrm{d}t, \tag{18}$$

where u is a uniform deviate (a uniformly-distributed number in the range $0 \leq u < 1$). If numerical root finding is required, then Newton-Raphson is a suitable method (*e.g.* Press *et al.* 1992), and in that case it is worth noting that

$$F'(\tau) = \lambda \left[E^*(t_e), t_e \right], \tag{19}$$

where $t_e = t_s + \tau$.

Once the waiting time τ has been generated, the jump may be simulated. The energy before the jump is $E_e = E^*(t_e)$, the end-energy of the deterministic trajectory. The size ΔE of the jump may be determined by generating a random variable from the distribution $h(\Delta E, E_e, t_e)$, which is defined by Equation (15). A value ΔE may be obtained by the usual technique of transforming a uniform deviate to a random variable from the required distribution (Press *et al.*, 1992). Once ΔE is calculated, a new start energy $E_s = E_e - \Delta E$ is specified at time t_e just after the jump, and the whole process may then be repeated. This procedure can be repeated an arbitrary number of times, to give a simulated time history of energy $E(t)$ for the system over an arbitrary number of jumps. Provided Equations (17) and (18) are straightforward to evaluate, the process involves relatively little computational expense.

3.2. GAUSSIAN TEST CASE

To illustrate the method, consider the "Gaussian" test case discussed in Wheatland and Glukhov (1998) and Wheatland (2008), namely the case with $\beta(E,t) = \beta_0$ and $\alpha(E, E', t) = \alpha_0$ (where α_0 and β_0 are constants). In that case the solution to the steady state master equation is

$$P(E) = aE \mathrm{e}^{-\frac{1}{2}aE^2}, \tag{20}$$

with $a = \alpha_0 / \beta_0$, and from Equation (6) the frequency-energy distribution for jumps is also a Gaussian:

$$\mathcal{N}(E) = \alpha_0 \mathrm{e}^{-\frac{1}{2}aE^2}. \tag{21}$$

From Equation (3) the total rate of events is $\lambda(E) = \alpha_0 E$, and from Equation (4) the mean total rate is $\langle \lambda \rangle = (\alpha_0 \beta_0)^{1/2}$. Using the method outlined in Wheatland (2008), the waiting-time distribution is also a Gaussian:

$$p_\tau(\tau) = \left(\frac{2\alpha_0 \beta_0}{\pi} \right)^{1/2} \mathrm{e}^{-\frac{1}{2}\alpha_0 \beta_0 \tau^2}. \tag{22}$$

To simulate the Gaussian test case using the Monte-Carlo approach, note that the solution to Equation (17) with $\beta(E,t) = \beta_0$ and with starting energy E_s at time t_s is

$$E^*(t) = E_s + \beta_0 (t - t_s), \tag{23}$$

and we have $\lambda(E) = \alpha_0 E$, so

$$\lambda[E^*(t)] = \alpha_0 \left[E_s + \beta_0 (t - t_s) \right]. \tag{24}$$

Equation (18) evaluates to

$$F(\tau) = \ln(1 - u) + \alpha_0 E_s \tau + \frac{1}{2}\alpha_0\beta_0\tau^2,$$ (25)

and taking the positive root of this quadratic function gives

$$\tau = \frac{E_s}{\beta_0}\left[\left(1 + \frac{2}{aE_s^2}\ln\frac{1}{1-u}\right)^{1/2} - 1\right].$$ (26)

For this case the distribution of jump amplitudes, from Equation (15), is given by

$$h(\Delta E, E) = \frac{1}{E}$$ (27)

for $0 \leq \Delta E \leq E$. The jump energies are uniformly distributed on $(0, E)$, and a jump may be generated from a uniform deviate u using $\Delta E = Eu$. Finally, the mean energy

$$\langle E \rangle = \left(\frac{\pi}{2a}\right)^{1/2}$$ (28)

provides a suitable starting energy for simulation.

Figure 1 illustrates a Monte-Carlo solution of the Gaussian test case using Equations (23)–(28), for the choices $\alpha_0 = 0.01$ and $\beta_0 = 1$. The upper panel in the figure shows the time history of system energy for the simulation for 25 jumps, and the lower panel shows the corresponding event energies *versus* time. The energy of the system grows linearly with time between jumps, and the jumps occur with a rate which increases linearly with energy. The jump sizes are uniformly distributed, up to the current energy of the system.

Figure 2 illustrates the Monte-Carlo solution of the Gaussian test case with the same parameters ($\alpha_0 = 0.01$ and $\beta_0 = 1$) for 5000 waiting times and jumps, and compares the results with the analytic expressions. The left-hand panel shows the histogram of the system energy, and the right-hand panel shows the histogram of waiting times. The corresponding analytic distributions $P(E)$ and $p_\tau(\tau)$, given by Equations (20) and (22) respectively, are shown by the solid curves. The histogram of system energy was obtained by sampling the simulated time history of energy $E(t)$ at 5000 random times, uniformly distributed over the duration of the simulation. These results illustrate the application of the Monte-Carlo approach, and confirm that it reproduces the analytic results.

3.3. FLARE-LIKE CASES

Next we consider the flare-like cases corresponding to Equation (8), from Wheatland (2008). For those case the total rate of flaring is given by Equation (11), and the energy supply rate is $\beta = \beta_0$, a constant. If the last event is at $t = t_s$, when the energy is E_s, then the subsequent deterministic trajectory in energy (prior to the next jump) is given by Equation (23). Using this result and Equation (11),
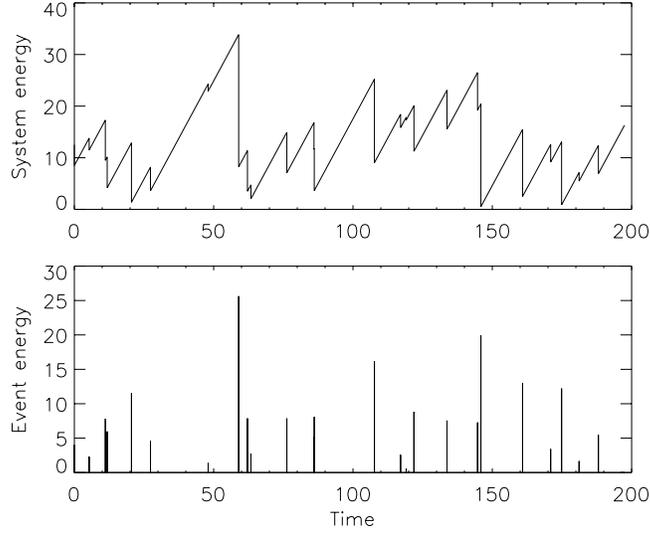
Figure 1. Monte-Carlo solution of the Gaussian test case with $\alpha_0 = 0.01$ and $\beta_0 = 1$, with 25 jump transitions and waiting times. The upper panel shows the system energy *versus* time, and the lower panel shows the event energies *versus* time.
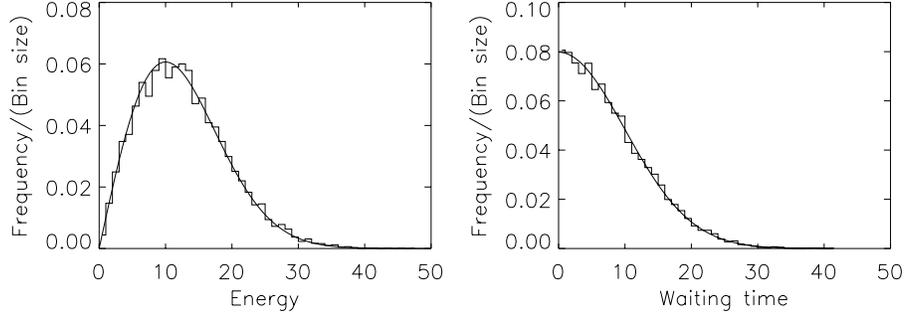
Figure 2. Monte-Carlo solution of the Gaussian test case, involving 5000 jump transitions, and parameter values $\alpha_0 = 0.01$, $\beta_0 = 1$. The histogram in the left-hand panel shows the distribution of system energy, and the histogram in the right-hand panel shows the distribution of waiting times. The corresponding analytic results are shown in the two panels by solid curves.

Equation (18) evaluates to

$$F(\tau) = \ln(1 - u) \ + \ \frac{\alpha_0/\beta_0}{\gamma - 1} \left\{ \frac{E_c^{-\gamma+1}}{\delta + 1} \left[(E_s + \beta_0\tau)^{\delta+1} - \epsilon^{\delta+1} \right] \right.$$
$$\left. - \ \frac{1}{\delta - \gamma + 2} \left[(E_s + \beta_0\tau)^{\delta-\gamma+2} - \epsilon^{\delta-\gamma+2} \right] \right\}, \qquad (29)$$

where $\epsilon = E_s$ if $E_s \geq E_c$, and $\epsilon = E_c$ if $E_s < E_c$. In this case numerical root finding is required, and for the application of Newton-Raphson it is helpful to note from Equation (19) that

$$F'(\tau) = \frac{\alpha_0}{\gamma - 1} \left(E_s + \beta_0\tau\right)^{\delta} \left[E_c^{-\gamma+1} - \left(E_s + \beta_0\tau\right)^{-\gamma+1}\right]. \tag{30}$$

The distribution of jump energies defined by Equation (15) is

$$h(\Delta E, E) = \frac{(\gamma - 1)(\Delta E)^{-\gamma+1}}{E_c^{-\gamma+1} - E^{-\gamma+1}} \tag{31}$$

for $E_c \leq \Delta E \leq E$. A variable with this distribution may be generated from a uniform deviate u for a given E using the transformation

$$\Delta E = \left[E_c^{-\gamma+1} - u\left(E_c^{-\gamma+1} - E^{-\gamma+1}\right)\right]^{-1/(\gamma-1)}. \tag{32}$$

A suitable starting energy for a simulation is provided by Equation (10).

Following Wheatland and Glukhov (1998) and Wheatland (2008), it is useful to non-dimensionalize, by introducing

$$\overline{E} = \frac{E}{E_c}, \quad \overline{t} = \frac{\beta_0 t}{E_c}, \tag{33}$$

and

$$\overline{r} = \frac{\alpha_0 E_c^{\delta-\gamma+2}}{\beta_0}. \tag{34}$$

Equations (29) and (30) become

$$F(\overline{\tau}) = \ln(1 - u) \ + \ \frac{\overline{r}}{\gamma - 1}\left\{\frac{1}{\delta + 1}\left[\left(\overline{E}_s + \overline{\tau}\right)^{\delta+1} - \overline{\epsilon}^{\delta+1}\right]\right.$$
$$\left. - \ \frac{1}{\delta - \gamma + 2}\left[\left(\overline{E}_s + \overline{\tau}\right)^{\delta-\gamma+2} - \overline{\epsilon}^{\delta-\gamma+2}\right]\right\} \tag{35}$$

where $\overline{\epsilon} = \overline{E}_s$ if $\overline{E}_s \geq 1$, and $\overline{\epsilon} = 1$ if $\overline{E}_s < 1$, and

$$F'(\overline{\tau}) = \frac{\overline{r}}{\gamma - 1}\left(\overline{E}_s + \overline{\tau}\right)^{\delta}\left[1 - \left(\overline{E}_s + \overline{\tau}\right)^{-\gamma+1}\right], \tag{36}$$

respectively. The transformation used to generate jump energies is

$$\Delta\overline{E} = \left[1 - u\left(1 - \overline{E}^{-\gamma+1}\right)\right]^{-1/(\gamma-1)}, \tag{37}$$

and the starting energy is

$$\langle\overline{E}\rangle \approx \left(\frac{2 - \gamma}{\overline{r}}\right)^{1/(\delta+2-\gamma)}. \tag{38}$$

The parameters δ and $\overline{r}$ define the specific model being solved. Equation (38) implies that $\overline{r} < \frac{1}{2}$ is required for $\langle \overline{E} \rangle > 1$. Smaller values of $\overline{r}$ lead to larger values of $\langle \overline{E} \rangle$ and hence more decades of power-law behavior in the frequency-energy distribution, as explained in Section 2.2. Many decades of power-law behavior are observed for flares on the Sun, implying a small value of $\overline{r}$.

As an example of applying Equations (35) – (38), we consider the case $\delta = 0$, from Wheatland and Glukhov (1998). Figure 3 shows the results of a Monte-Carlo solution with $\delta = 0$ and $\overline{r} = 0.02$. The upper panel shows the time history of the energy of the model active region over the first 50 jumps, and the lower panel shows the corresponding flare energies *versus* time (with a logarithmic scale). The mean energy of the system is $\langle \overline{E} \rangle = 625$, which is the starting energy for the simulation. Figure 3 illustrates the character of the flare-like models. The active-region energy grows linearly with time between flares, flare sizes are power-law distributed, and the total flaring rate is approximately constant, since $\overline{E} \gg 1$. During this period of time only relatively small flares occurred, with the largest event having energy close to 100 in non-dimensional units.
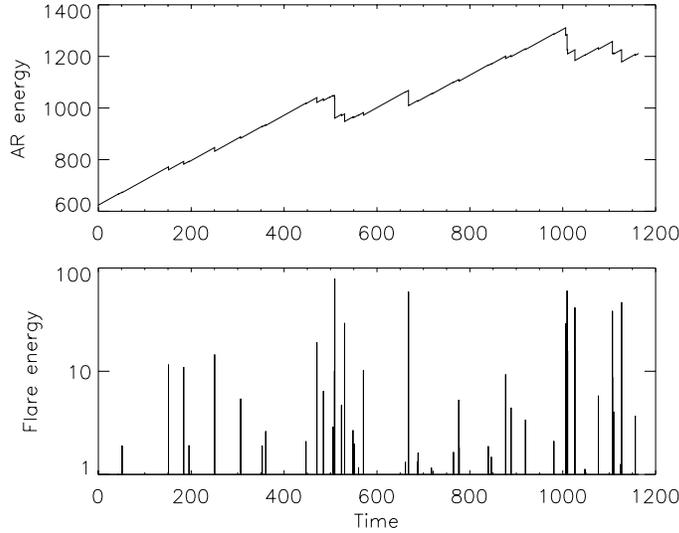
Figure 3. Monte-Carlo solution of the flare-like case from Wheatland and Glukhov (1998), with $\delta = 0$ and $\overline{r} = 0.02$. The upper panel shows the active-region energy *versus* time, and the lower panel shows the flare energy *versus* time, for a period of time including 50 jump transitions.

Figure 4 illustrates the Monte-Carlo solution with the same parameters ($\delta = 0$ and $\overline{r} = 0.02$) for 3×10^4 waiting times and jump transitions, and compares the results with direct solution of the master equation. The upper-left panel shows the time history of the energy of the system, with the mean energy $\langle \overline{E} \rangle = 625$ shown by a horizontal line, which is also indicated by an arrow near the left-hand axis of the panel. The upper-right panel shows the histogram of the energy of the system, obtained by sampling the simulated time history of energy at 3×10^4

random times. The mean energy is shown by a solid vertical line. The solid curve is the distribution obtained by solving the master equation in the steady state, using the method in Wheatland (2008). The lower-left panel shows the histogram of waiting times, in a log-linear representation, together with the waiting-time distribution obtained from the solution to the master equation (solid curve). The lower-right panel shows the flare frequency-energy histogram, together with the distribution obtained from the solution to the master equation (solid curve), and the mean energy (solid vertical line). The Monte-Carlo solutions agree with the direct solution of the master equation. These results confirm the finding in Wheatland (2008) that the waiting-time distribution is essentially exponential in this case.
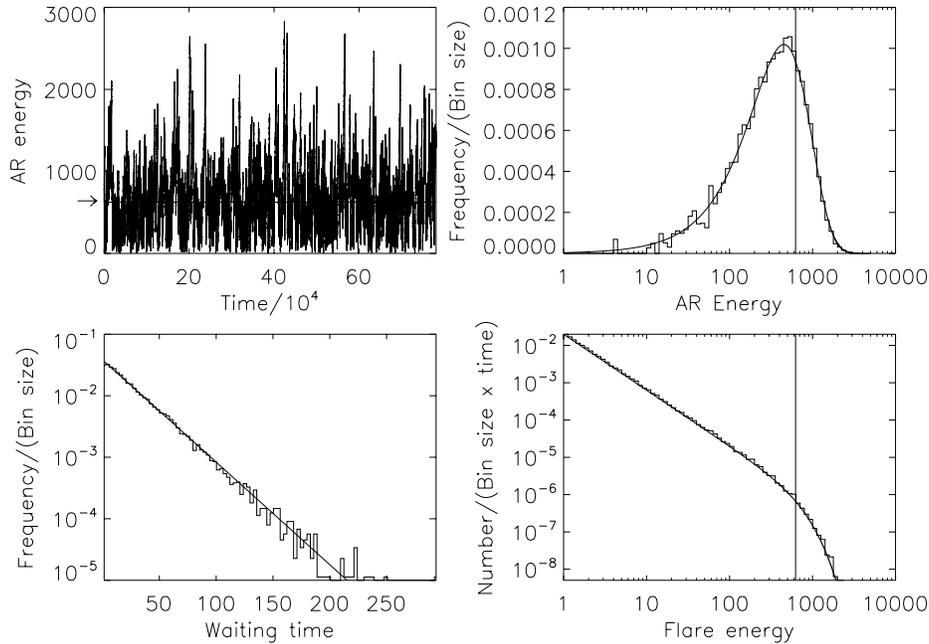
Figure 4. Monte-Carlo solution of the flare-like case from Wheatland and Glukhov (1998), involving 3×10^4 jump transitions, and the parameter value $\overline{r} = 0.02$. The figure shows the active-region energy *versus* time (upper left), and histograms of: the active-region energy (upper right); the waiting-time distribution (lower left); and the flare frequency-energy distribution (lower right). The corresponding results obtained by solving the master equation in the steady state are shown by solid curves. The active-region mean energy is indicated by an arrow near the left-hand axis of the upper-left panel, and is shown by a solid vertical line in the two panels on the right.

The comparison in Figure 4 illustrates the computational advantage of the Monte-Carlo method over direct solution of the master equation. The results shown by the solid curves in Figure 4 require the solution of a linear system in 5000 unknowns, to obtain sufficient energy resolution to ensure accuracy. By

comparison, the Monte-Carlo solution requires the simulation of 3×10^4 waiting times and jump transitions, but each of these calculations is simple. As a result the Monte-Carlo method is substantially faster than the linear solution.

3.4. WAITING-TIME DISTRIBUTIONS FOR FLARE-LIKE CASES

In Wheatland (2008) it was shown using numerical solutions of the master equation that the flare-like models with $\delta = 0$ and $\delta = 1$ exhibit approximately Poisson (exponential) waiting-time distributions, for certain choices of the non-dimensional ratio $\overline{r} = \alpha_0 E_c^{\delta-\gamma+2}/\beta_0$ of transition rates to energy-supply rate [in Wheatland (2008) this ratio was labelled $\overline{\alpha}_0$, or just α_0, when the bar was dropped]. These results are briefly discussed in Section 2.2. However, the results also showed some departure from the simple Poisson distribution. In this section we further investigate the behavior of the models and in particular the waiting-time distributions, using Monte-Carlo solutions.

Figure 5 illustrates three solutions for the case $\delta = 0$. Each solution involves 3×10^4 waiting times and jump transitions. The upper row in Figure 5 shows the flare frequency-energy distributions in a log-log representation, and the lower row shows the corresponding waiting-time distributions, in a log-linear representation. The left-hand pair of distributions is for $\overline{r} = 0.5$, the center pair is for $\overline{r} = 0.05$, and the right-hand pair is for $\overline{r} = 0.005$. The solid vertical lines in the frequency-energy distributions show the approximation to the mean energy $\langle \overline{E} \rangle$ given by Equation (38). The three choices of $\overline{r}$ shown correspond to values $\langle \overline{E} \rangle = 1$, $\langle \overline{E} \rangle = 10^2$, and $\langle \overline{E} \rangle = 10^4$. The solid lines on the waiting-time distributions show the exponential form $\overline{\lambda}_m e^{-\overline{\lambda}_m \overline{\tau}}$, where $\overline{\lambda}_m$ is the overall mean rate of events, *i.e.* the number of events divided by the total time (non-dimensionalised). The upper row of Figure 5 confirms that the frequency-energy distribution is a power law with index γ below a roll-over set by the largest energy the system is likely to attain, which may be roughly approximated by $\langle \overline{E} \rangle$. For smaller values of $\overline{r}$, the system attains larger energies, as flaring is less frequent. The lower row of Figure 5 shows that the waiting-time distribution becomes exponential as $\langle \overline{E} \rangle$ increases (or as $\overline{r}$ decreases). This may be understood using the argument given in Section 2.2: for $\overline{r} \ll 1$, the energy $\overline{E}$ of the system satisfies $\overline{E} \gg 1$, in which case the approximation of Equation (12) applies, and the total rate of flaring $\overline{\lambda}(\overline{E})$ is then independent of $\overline{E}$.

Figure 6 illustrates three solutions for the case $\delta = 1$, again with 3×10^4 waiting times and jump transitions. The format of the figure is the same as for Figure 5, and the values of $\overline{r}$ for the three cases are chosen so that the values of $\langle \overline{E} \rangle$ [using the approximation of Equation (38)] are the same, *i.e.* $\langle \overline{E} \rangle = 1$ (left), $\langle \overline{E} \rangle = 10^2$ (center), and $\langle \overline{E} \rangle = 10^4$ (right). The corresponding values of $\overline{r}$ are given above the three rows in the figure. The upper row of Figure 6 shows the expected power-law behavior below an upper roll-over given approximately by $\langle \overline{E} \rangle$. The lower row of Figure 6 shows that the waiting-time distribution is approximately exponential for $\langle \overline{E} \rangle = 10^2$, but for $\langle \overline{E} \rangle = 10^4$ there is an excess of large waiting times by comparison with the exponential form. Referring again to the argument in Section 2.2, for $\overline{r} \ll 1$ we expect $\overline{E} \gg 1$, in which case the total flaring rate varies approximately as $\overline{\lambda}(\overline{E}) \propto \overline{E}$. The linear variation in mean
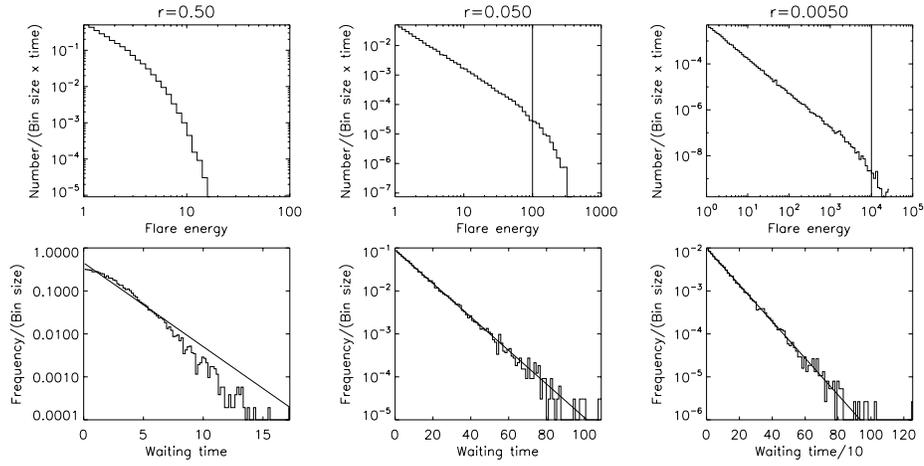
Figure 5. The flare frequency-energy distributions (upper row) and flare waiting-time distributions (lower row) for the flare-like case with $\delta = 0$. The left-hand pair of distributions is for $\langle\overline{E}\rangle \approx 1$ ($\overline{r} = 0.5$), the center pair is for $\langle\overline{E}\rangle \approx 10^2$ ($\overline{r} = 5 \times 10^{-2}$), and the right-hand pair is for $\langle\overline{E}\rangle \approx 10^4$ ($\overline{r} = 5 \times 10^{-3}$).
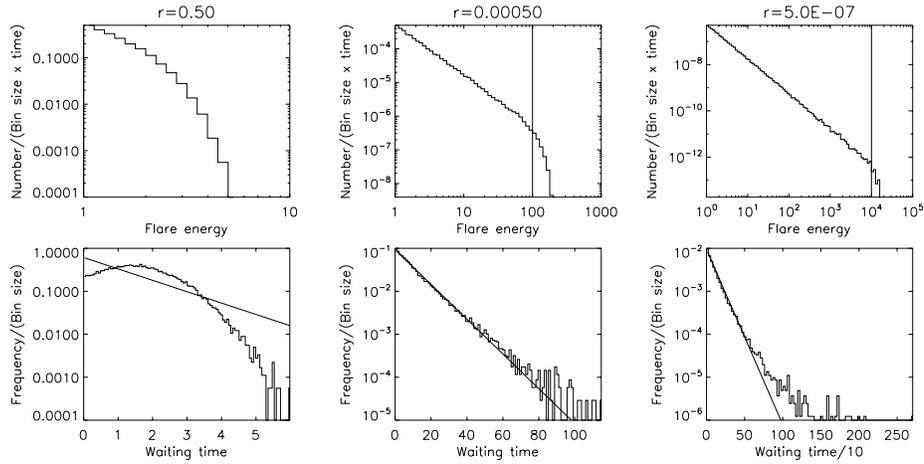
Figure 6. The flare frequency-energy distributions (upper row) and flare waiting-time distributions (lower row) for the flare-like case with $\delta = 1$. The left-hand pair of distributions is for $\langle\overline{E}\rangle = 1$ ($\overline{r} = 0.5$), the center pair is for $\langle\overline{E}\rangle = 10^2$ ($\overline{r} = 5 \times 10^{-4}$), and the right-hand pair is for $\langle\overline{E}\rangle = 10^4$ ($\overline{r} = 5 \times 10^{-7}$).

flaring rate with energy leads to some departure from the simple exponential form, with the departure becoming more significant as $\overline{r}$ decreases.

Figure 7 illustrates three solutions for the case $\delta = 2$, again with 3×10^4 waiting times and jump transitions. The format of the figure is the same as for Figures 5 and 6, with the values of $\overline{r}$ again corresponding to approximate mean energies $\langle\overline{E}\rangle = 1$ (left), $\langle\overline{E}\rangle = 10^2$ (center), and $\langle\overline{E}\rangle = 10^4$ (right). The results
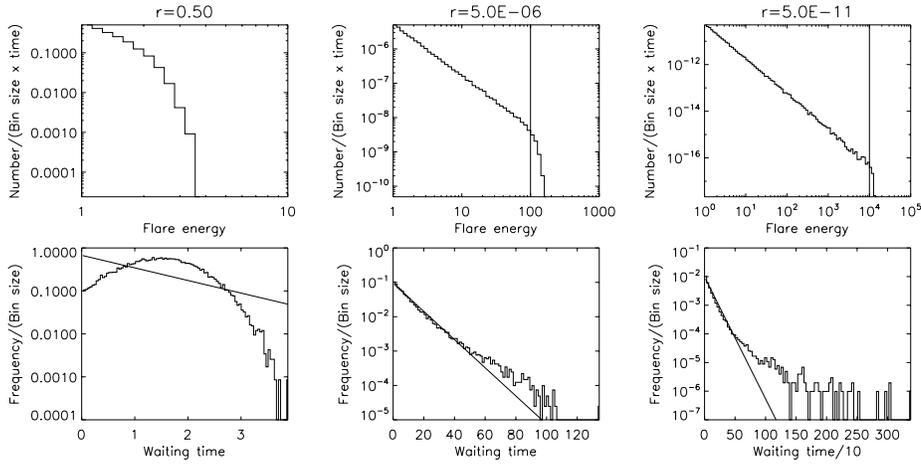
Figure 7. The flare frequency-energy distributions (upper row) and flare waiting-time distri-
butions (lower row) for the flare-like case with $\delta = 2$. The left-hand pair of distributions is for
$\langle \overline{E} \rangle = 1$ ($\overline{r} = 0.5$), the center pair is for $\langle \overline{E} \rangle = 10^2$ ($\overline{r} = 5 \times 10^{-6}$), and the right-hand pair is
for $\langle \overline{E} \rangle = 10^4$ ($\overline{r} = 5 \times 10^{-11}$).

for the frequency-energy distribution (upper row) are as expected, with power-
law behavior below an upper roll-over given approximately by $\langle \overline{E} \rangle$. The results
for the waiting-time distribution are similar to the case $\delta = 1$, but are more
pronounced. For $\langle \overline{E} \rangle = 10^2$ there is very approximate exponential behavior, with
some excess of large waiting times. For $\langle \overline{E} \rangle = 10^4$ there is substantial departure
from the exponential model, with a pronounced excess of large waiting times.
Using the argument in Section 2.2, we expect approximate $\propto \overline{E}^2$ dependence of
the total flaring rate for $\overline{E} \gg 1$. This variation in the mean flaring rate with
energy leads to the departure from the exponential form.

The results shown in Figures 5–7 suggest that the $\delta = 0$ model may be the
preferred flare-like solution. The flare frequency-energy distribution is observed
to be a power law over many decades in energy, which implies $\overline{r} \ll 1$. The models
with $\delta \neq 0$ exhibit significant departure from Poisson waiting-time statistics for
$\overline{r} \ll 1$. However, it is not clear that any such departure is observed for flares
on the Sun: some active regions that produce very large flares appear to exhibit
simple Poisson waiting-time statistics (Moon *et al.*, 2001; Wheatland, 2001).

The variation in total flaring rate with energy of the system for the cases with
$\delta \neq 0$ also implies observable consequences. For example, if we pick out "large"
events from a simulation ensemble with $\delta \neq 0$ and plot the waiting time before
the event *versus* the waiting time after the event, then we expect that the waiting
times after the event will tend to be larger than the waiting times before, since
large events deplete the system energy, and hence reduce the total rate. Figure 8
illustrates this effect. The figure is constructed using the simulation shown in
Figure 7 with $\delta = 2$ and $\langle \overline{E} \rangle = 10^4$, and the threshold for a large event is chosen
to be $0.2\langle \overline{E} \rangle$. The solid line is the line of equality of the two waiting times. As
expected, the waiting times after the large events tend to be larger than the

waiting times before the event (more points lie below the line of equality than above). No such effect is observed when a similar plot is constructed for the model with $\delta = 0$ and $\langle \overline{E} \rangle = 10^4$. This effect is not observed for flares on the Sun (Wheatland, Sturrock, and McTiernan, 1998; Wheatland, 2001).
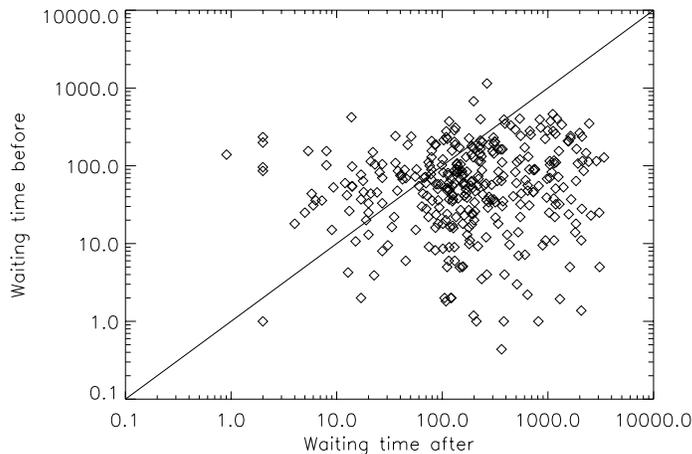
Figure 8. Plot of the waiting time before an event, *versus* the waiting time after an event, for all events larger than $0.2\langle \overline{E} \rangle$, for the simulation with $\delta = 2$ and $\langle \overline{E} \rangle = 10^4$ shown in Figure 7.

4. Conclusions

This paper presents a Monte-Carlo method for solving the stochastic model for active region energy presented in Wheatland and Glukhov (1998) and Wheatland (2008), which in particular is suited to solving the flare-like cases in those papers. The method numerically solves the stochastic differential equation describing the system, rather than the equivalent master equation, and provides a computationally-efficient approach to the problem. The method is demonstrated on a simple Gaussian test, and is compared with a direct solution of the steady-state master equation for a flare-like case from Wheatland and Glukhov (1998).

The method is used to further investigate the class of flare-like models from Wheatland (2008), which feature constant energy-supply rates β_0 and flare transition rates of the form

$$\alpha(E, E') = \alpha_0 E^\delta (E - E')^{-\gamma} \theta(E - E' - E_c), \qquad (39)$$

where α_0 is a constant, and E_c is a low-energy cutoff. The index $\gamma = 1.5$ is the observed flare frequency-energy power law index, and δ is a positive constant (we consider the cases $\delta = 0$, $\delta = 1$, and $\delta = 2$). The emphasis in the investigation is on the waiting-time distributions for these models, and their adherance

to/departure from a Poisson (exponential) form, as a function of δ and of the dimensionless ratio $\overline{r} = \alpha_0 E_c^{\delta-\gamma+2}/\beta_0$. The models require small values of $\overline{r}$ to produce flares with a frequency-energy distribution exhibiting a power law over many decades [a lower bound to the departure from power-law behavior is set by the estimate of the mean energy $\langle \overline{E} \rangle \approx [(2-\gamma)/\overline{r}]^{1/(\delta+2-\gamma)}$]. For the $\delta = 0$ model it is found that the waiting-time distribution becomes a close approximation to a simple exponential for small $\overline{r}$. This may be explained in terms of the total rate of flaring becoming constant for large $\overline{E}$, which applies when $\overline{r} \ll 1$. For the $\delta = 1$ and $\delta = 2$ models the waiting-time distribution is approximately exponential for intermediate values of $\overline{r}$, but exhibits an excess of large waiting times for $\overline{r} \ll 1$. This result may make the $\delta = 0$ case the preferred flare-like solution, since it is unclear that any such departure is observed for flares on the Sun. Also, the dependence of the total flaring rate on the active-region energy for the $\delta = 1$ and $\delta = 2$ models implies variations in flare rate with flare occurrence which do not appear to be observed on the Sun.

It is interesting to reconsider the correspondence between the stochastic model and the avalanche model for flares (Lu and Hamilton, 1991; Charbonneau *et al.*, 2001), in light of the new results. The investigation in this paper excludes the possibility of a stochastic model with transition rates of the form of Eq. (39) with $\delta \neq 0$, which simultaneously exhibits a wide range of flare energies and has uncorrelated waiting times. This is due to large flares changing the system energy and hence total flaring rate significantly. The choice for the transition rates was motivated in part by the avalanche model (as outlined in Section 2.2). Avalanche models exhibit power-law frequency-energy distributions over many decades, and they have uncorrelated waiting times (Wheatland, Sturrock, and McTiernan, 1998). However, in avalanche models the largest flares deplete only a small fraction of of the avalanche grid "energy" (see *e.g.* Fig. 3 in Charbonneau *et al.*, , 2001). The discrepancy between the two pictures might be due to different definitions of energy (the avalanche model "energy" may correspond to free energy plus background magnetic energy unavailable for flares). Another possibility is that the $\delta = 0$ model provides the closest match to the avalanche picture. A more careful analysis of the correspondence between the two models is needed to resolve this point.

The Monte-Carlo approach has several advantages over solution of the master equation. First, as discussed in Section 3.3, the Monte-Carlo solution is numerically simple to implement and computationally efficient. Second, as highlighted by Figure 8, since the Monte-Carlo approach produces an ensemble of flare events, it permits detailed investigation of event statistics. A third advantage of the Monte-Carlo method is that it permits solution of the model in time-dependent situations. In principle solutions may be constructed for arbitrary time variation of the rates $\beta(E, t)$ and $\alpha(E, E', t)$. The methods of solution of the master equation presented in Wheatland and Glukhov (1998) and Wheatland (2008) apply only in the steady state, and in particular the method of obtaining the waiting-time distribution requires a steady state. As discussed in Section 1, time variation in observed flaring rates plays a role in determining the observed waiting-time distribution, so it is of interest to consider time-dependent models. These models will be addressed in future work.

It is possible to construct more general stochastic models for active-region energy. Active regions may lose energy by mechanisms other than flaring, *e.g.* due to slow ohmic dissipation of electric currents. If the energy loss is considered to be deterministic, and smaller in magnitude than the energy input rate, then $\beta(E,t)$ in the present model may be interpreted as a *net* energy-supply rate, and the model may be considered to already accommodate energy losses of this kind. If the energy loss is assumed to occur via small random decrements, then a suitable model may be to include a Fokker-Planck (diffusion) term in the master equation, describing continual small random increases and decreases in energy. (The increases may correspond to fluctuations in the energy supply rate.) A more general form for the jump-transition master equation, sometimes called the Chapman-Kolmogorov equation (Gardiner, 2004) includes drift (representing deterministic energy input or loss), diffusion (small random input or loss), and jump transitions. An active-region model of this form was briefly discussed in Wheatland (2008). In the context of the Monte-Carlo approach, the diffusion term corresponds to a Wiener process, and a different method of solution of the stochastic DE is then required.

Models of the kind presented in this paper are difficult to test in detail against flare observations because of the difficulties associated with determining the free energy of active regions, and the rate of energy supply to active regions. However, we note that improved solar observations (and analysis techniques) may eventually provide such information. Independent of this, the models provide important qualitative checks on our understanding of energy balance in solar active regions. For example, as noted in Section 2.2, it has proven difficult to identify choices other than the flare-like ones investigated here that produce suitable power-law flare frequency-energy distributions. The models are also of intrinsic interest because of their description of a dynamical balance involving scale-free transitions, and it is possible that they provide suitable descriptions of a variety of other physical systems exhibiting power-law behavior.

References

Aschwanden, M.J., Dennis, B.R., Benz, A.O.: 1998, *Astrophys. J.* **497**, 972.
Baiesi, M., Paczuski, M., Stella, A.L.: 2006, *Phys. Rev. Lett.* **96**, 051103.
Barnes, G., Leka, K.D.: 2008, *Astrophys. J.* **688**, L107.
Barnes, G., Leka, K.D., Schumer, E.A., Della-Rose, D.J.: 2007, *Space Weather* **5**, 9002.
Biesecker, D.A.: 1994, *Ph.D. Thesis*, Univ. New Hampshire
Boffetta, G., Carbone, V., Giuliani, P., Veltri, P., Vulpiani, A.: 1999, *Phys. Rev. Lett.* **83**, 4662.
Buchlin, E., Galtier, S., Velli, M.: 2005, *Astron. Astroph.* **436**, 355.
Charbonneau, P., McIntosh, S.W., Liu, H.-L., Bogdan, T.J.: 2001, *Solar Phys.* **203**, 321.
Crosby, N., Aschwanden, M., Dennis, B.: 1993, *Adv. Space Res.* **13**, 179.
Daly, E., Porporato, A.: 2007, *Phys. Rev. E* **75**, 011119.
Gardiner, C.W.: 2004, *Handbook of Stochastic Methods*, Springer, Berlin.
Georgoulis, M.K., Rust, D.M.: 2007, *Astrophys. J.* **661**, L109.
Hudson, H.S.: 1991, *Solar Phys.* **133**, 357.

Hudson, H.S.: 2007, *Astrophys. J.* **663**, L45.

Kubo, Y.: 2008, *Solar Phys.* **248**, 85.

Kucera, T.A., Dennis, B.R., Schwartz, R.A., Shaw, D.: 1997, *Astrophys. J.* **475**, 338.

Lepreti, F., Carbone, V., Veltri, P.: 2001, *Astrophys. J.* **555**, L133.

Lu, E.T., Hamilton, R.J.: 1991, *Astrophys. J.* **380**, L89.

McIntosh, P.S.: 1990, *Solar Phys.* **125**, 251.

Moon, Y.-J., Choe, G.S., Yun, H.S., Park, Y.D.: 2001, *J. of Geophys. Res.* **106**, 29951.

Moon, Y.-J., Choe, G.S., Park, Y.D., Wang, H., Gallagher, P.T., Chae, J., Yun, H.S., Goode, P.R.: 2002, *Astrophys. J.* **574**, 434.

Paczuski, M., Boettcher, S., Baiesi, M.: 2005, *Phys. Rev. Lett.* **95**, 181102.

Pearce, G., Rowe, A.K., Yeung, J.: 1993, *Astrophysics and Space Science* **208**, 99.

Press, W.H., Teukolsky, S.A., Vetterling, W.T., Flannery, B.P.: 1992, *Numerical Recipes in C: The Art of Scientific Computing*, 2nd ed., Cambridge: University Press.

Rosner, R., Vaiana, G.S.: 1978, *Astrophys. J.* **222**, 1104.

Sammis, I., Tang, F., Zirin, H.: 2000, *Astrophys. J.* **540**, 583.

Schrijver, C.J.: 2007, *Astrophys. J.* **655**, L117.

van Kampen, N.G.: 1992, *Stochastic Processes in Physics and Chemistry (Revised and enlarged edition)*, Elsevier Science, Amsterdam.

Wheatland, M.S.: 2000, *Astrophys. J.* **532**, 1209.

Wheatland, M.S.: 2001, *Solar Phys.* **203**, 87.

Wheatland, M.S.: 2005, *Space Weather* **3**, 7003.

Wheatland, M.S.: 2008, *Astrophys. J.* **679**, 1621.

Wheatland, M.S., Craig, I.J.D.: 2006, *Solar Phys.* **238**, 73.

Wheatland, M.S., Glukhov, S.: 1998, *Astrophys. J.* **494**, 858.

Wheatland, M.S., Sturrock, P.A., McTiernan, J.M.: 1998, *Astrophys. J.* **509**, 448.